NIH Public Access
Author Manuscript
J Biomech. Author manuscript; available in PMC 2015 June 27.

Published in final edited form as:
J Biomech. 2014 June 27; 47(9): 2165–2172. doi:10.1016/j.jbiomech.2013.10.044.

Synthesis Rates and Binding Kinetics of Matrix Products in Engineered Cartilage Constructs Using Chondrocyte-Seeded Agarose Gels

Robert J. Nims, M.S.[1], **Alexander D. Cigan, M.S.**[1], **Michael B. Albro, Ph.D.**[2], **Clark T. Hung, Ph.D.**[1], and **Gerard A. Ateshian, Ph.D.**[1,2]

[1]Department of Biomedical Engineering, Columbia University, 1210 Amsterdam Avenue, MC 8904, 351 Engineering Terrace, New York, NY 10027

[2]Department of Mechanical Engineering, Columbia University, 500 West 120th Street, MC4703, 220 Mudd, New York, NY 10027

Abstract

Large-sized cartilage constructs suffer from inhomogeneous extracellular matrix deposition due to insufficient nutrient availability. Computational models of nutrient consumption and tissue growth can be utilized as an efficient alternative to experimental trials to optimize the culture of large constructs; models require system-specific growth and consumption parameters. To inform models of the [bovine chondrocyte]-[agarose gel] system, total synthesis rate (matrix accumulation rate + matrix release rate) and matrix retention fractions of glycosaminoglycans (GAG), collagen, and cartilage oligomeric matrix protein (COMP) were measured either in the presence (continuous or transient) or absence of TGF-β3 supplementation. TGF-β3's influence on pyridinoline content and mechanical properties was also measured. Reversible binding kinetic parameters were characterized using computational models. Based on our recent nutrient supplementation work, we measured glucose consumption and critical glucose concentration for tissue growth to computationally simulate the culture of a human patella-sized tissue construct, reproducing the experiment of Hung et al., (2003). Transient TGF-β3 produced the highest GAG synthesis rate, highest GAG retention ratio, and highest binding affinity; collagen synthesis was elevated in TGF-β3 supplementation groups over control, with the highest binding affinity observed in the transient supplementation group; both COMP synthesis and retention were lower than those for GAG and collagen. These results informed the modeling of GAG deposition within a large patella construct; this computational example was similar to previous experimental results without further adjustments to modeling parameters. These results suggest that these nutrient consumption and

© 2013 Elsevier Ltd. All rights reserved.

Corresponding author: Gerard A. Ateshian, Ph.D., Professor of Mechanical Engineering and Biomedical Engineering, Columbia University, 500 West 120th Street, MC 4703, New York, NY 10027 USA, Phone: 212-854-2966, Fax: 212-854-3304, ateshian@columbia.edu.

Publisher's Disclaimer: This is a PDF file of an unedited manuscript that has been accepted for publication. As a service to our customers we are providing this early version of the manuscript. The manuscript will undergo copyediting, typesetting, and review of the resulting proof before it is published in its final citable form. Please note that during the production process errors may be discovered which could affect the content, and all legal disclaimers that apply to the journal pertain.

Author Disclosure Statement
No competing financial interests exist.

NIH-PA Author Manuscript
NIH-PA Author Manuscript
NIH-PA Author Manuscript

NIH-PA Author Manuscript

NIH-PA Author Manuscript

NIH-PA Author Manuscript

matrix synthesis models are an attractive alternative for optimizing the culture of large-sized constructs.

Keywords

Tissue engineering; extracellular matrix; cartilage; growth; anatomical models

Introduction

Osteoarthritis (OA) is a debilitating disease causing significant pain and immobility as the cartilage of the diarthrodial joints degrades to expose the underlying bone. The low cellularity and avascular nature of adult articular cartilage contribute to the limited capacity of the tissue to heal from minor injuries and defects, eventually developing into symptomatic OA (Stockwell, 1979). Cartilage tissue engineering (CTE) is a promising strategy targeting the replacement of defective native cartilage with mechanically and biochemically similar engineered cartilage. In CTE, systems usually consist of a cell species embedded in a biocompatible polymeric scaffold (Langer and Vacanti, 1993). The scaffold maintains the cells in a three-dimensional environment with access to a nutrient rich culture media and retains the extracellular matrix (ECM) products synthesized by the cells. In particular, agarose is a well-characterized, bio-inert scaffold that shows great promise in CTE systems as chondrocytes elaborate a functional ECM when cultured in the 3D agarose environment, reaching native levels of glycosaminoglycans (Benya and Shaffer, 1982; Buschmann et al., 1992; Byers et al., 2008; Lima et al., 2007).

A remaining challenge in CTE is the development of clinically relevant-sized tissue constructs, which are required to repair the large surface defects (> 5 cm^2) present in symptomatic OA (Hung et al., 2003; Hung et al., 2004; Moisio et al., 2009). Engineered constructs of this size suffer from inhomogeneous ECM deposition as the transport of critical nutrients to the interior of the construct is hindered by consumption by peripheral cells. Lacking a homogenous and structural ECM, these constructs are unable to support physiologic loads and are therefore unlikely to function successfully upon implantation. In an effort to reduce ECM heterogeneity, strategies for enhancing nutrient transport have been employed such as direct media perfusion, dynamic mechanical loading, and the introduction of nutrient channels into the tissue (Bian et al., 2009; Buckley et al., 2009; Davisson et al., 2002a; Davisson et al., 2002b; Lima et al., 2007; Mauck et al., 2000). However, quantitative predictive methods for optimizing the culture of large-sized constructs remain unexplored.

An overarching aim of our research is to develop and implement continuum growth models to optimize the culture of large-sized constructs with sufficient nutrient availability for ECM deposition throughout the construct's interior. Such models may prove insightful and efficient in analyzing how nutrient distribution and ECM deposition are affected by culture conditions (Nikolaev et al., 2010; Obradovic et al., 2000; Sengers et al., 2004b, 2005; Zhou et al., 2008). System-specific CTE modeling requires knowledge of: (1) the nutrient(s) essential for cell viability and concentrations of the nutrient(s) necessary for tissue growth, (2) consumption rates of the nutrient(s), (3) matrix constituents critical to mechanical

NIH-PA Author Manuscript

NIH-PA Author Manuscript

NIH-PA Author Manuscript

integrity, and (4) synthesis rate and binding kinetics for essential ECM constituents. In cartilage, proteoglycans (PGs) and type II collagen are the major ECM structural components. PGs, predominantly consisting of aggregated glycosaminoglycans (GAG), contribute to the compressive stiffness while the fibrillar collagen network contributes to the tensile behavior (Jurvelin et al., 1988; Kempson et al., 1973). Pyridinoline cross-links between collagen fibrils act to retain and strengthen the PG-collagen network (Eyre and Wu, 2005; Williamson et al., 2003a; Williamson et al., 2003b). In addition, cartilage oligomeric matrix protein (COMP) is a high molecular weight (~500 kDa) matrix protein that may play a structural role in cartilage given its concentration (0.4% ww) in the tissue and binding affinity for both PGs and type II collagen (Chen et al., 2007; DiCesare et al., 1996; Hedbom et al., 1992; Rosenberg et al., 1998; Roughley, 2001).

Previously, we have identified that tissue growth is diminished at a glucose concentration of 7.5 mM as compared to 25 mM in the [bovine chondrocyte] – [agarose gel] system (Cigan et al., 2013). The present study, therefore, focuses on the remaining tasks of experimentally measuring ECM synthesis and retention to determine the matrix binding kinetics, measuring the rate of glucose consumption for this system, and refining the glucose concentration threshold required for ECM synthesis. The synthesis rates, retention fractions, and binding constants of GAG, collagen, and COMP were examined in the continuous and temporary (2 week) supplementation, as well as absence, of transforming growth factor β3 (TGF-β3) (Byers et al., 2008; Lima et al., 2007). Pyridinoline content was also assessed under the influence of TGF-β3. Biochemical composition was correlated to the mechanical properties to investigate the ECM's influence in the growth of this culture system. To preclude the confounding influence of heterogeneous nutrient availability present in large constructs, the experimental work of this study was performed with small constructs. To illustrate the utility of these parameters, we modeled the growth of a human patella-sized construct replicating the experiment by Hung et al. (2003), by incorporating glucose transport from a periodically refreshed bath, cellular glucose consumption, matrix synthesis based on glucose availability, and binding and release of matrix products.

Materials and Methods

Cell isolation, construct culture, mechanical characterization and biochemical analysis follow standard methods employed in our previous studies and are summarized in the Supplementary Material. Briefly, juvenile primary bovine chondrocytes were encapsulated in 2% agarose at a density of 30×10^6 cells/mL. Constructs (∅4 mm × 2.3 mm thick) were cultured in chemically defined chondrogenic media. Media were supplemented with 10 ng/mL TGF-β3 (R&D Systems, Minneapolis, MN) for either the entire culture period (β3+ group) or for only the first 14 days of culture (β3– group). A control was cultured without TGF-β3 supplementation. Constructs were removed and characterized after 14, 28, and 45 days (n = 4 per group, time point).

Synthesis Rates and Retention Fractions

For each synthesized ECM constituent (GAG, collagen, COMP) two distinct rates were measured: (A) the constituent scaffold accumulation rate and (B) the constituent media

NIH-PA Author Manuscript

NIH-PA Author Manuscript

NIH-PA Author Manuscript

release rate. The scaffold mass accumulation rate, m_c, was the slope of the linear regression of the mass of matrix within each construct (normalized to the construct day 0 reference volume) over the culture period (typical data set and linear regression shown in Figure 1A). The media mass release rate, m_m, was the slope of the linear regression of the mass of matrix released into the media (normalized to the construct day 0 volume) over the culture period (typical data set and linear regression shown in Figure 1B). The linear regressions for the β3+ and control groups were calculated over the entire 45-day culture period (days 0 to 45) and the regressions for the β3− group were calculated after discontinuing TGF-β3 supplementation (days 14 to 45). The total synthesis rate was the sum of m_c and m_m. The retention ratio, R_c, of each matrix constituent was calculated by dividing m_c by the total synthesis rate:

$$R_c = \frac{m_c}{m_c + m_m} \quad (1)$$

The uncertainties of both the total synthesis rates and retention ratios were calculated according to standard uncertainty analysis from the standard deviations associated with the linear regression fits.

Binding Parameters

The reversible binding kinetics of each matrix constituent were assessed based on the following assumptions: the synthesis rate was based on experimental results; each constituent was synthesized in soluble form and bound reversibly according to the law of mass action; when in soluble form, matrix products underwent Fickian transport with a diffusivity negligibly altered by matrix deposition; soluble matrix products diffused out of the construct into a well-mixed bath; there were no nutrient limitations in these small constructs; electric charge effects were neglected; construct swelling as a result of matrix growth was also neglected. All model simulations were performed in the open-source finite element code FEBio (www.febio.org), customized for this application (Ateshian, 2007; Ateshian et al., 2013; Maas et al., 2012). Models consisted of a construct (∅4 mm × 2.3 mm thick, cell density: 30×10^6 cells/mL) in a 0.5 mL bath, similar to the day 0 experimental conditions (Figure S1A in Supplementary Material). The governing equation for soluble matrix product was the mass balance relation in the presence of chemical reactions,

$$\partial c/\partial t + \mathrm{div}\mathbf{j} = \hat{c} \quad (2)$$

where c is the solute molar concentration and $\mathbf{j} = -D\mathrm{grad}c$ is the molar flux of the solute relative to the construct solid matrix, with D representing the diffusivity. Here, $\hat{c}$ is the net rate of molar supply to the soluble constituent from chemical reactions, combining synthesis and reversible binding according to $\hat{c} = \hat{c}_{\mathrm{syn}} + \hat{c}_{\mathrm{rb}}$, where the synthesis rate $\hat{c}_{\mathrm{syn}}$ is prescribed from experimental measurements and was computed assuming a molar mass of 513 Da for GAG, 500 kDa for collagen, and 524 kDa for COMP. The reversible binding rate is

$$\hat{c}_{rb} = k_f\left[(c + K_d)c_b - N_t c\right] \quad (3)$$

NIH-PA Author Manuscript

NIH-PA Author Manuscript

NIH-PA Author Manuscript

Here, k_f is the forward reaction rate, k_r is the reverse reaction rate, $K_d = k_r/k_f$ is the dissociation constant, N_t is the total binding site concentration, and c_b is the concentration of bound matrix product whose temporal evolution is given by $dc_b / dt = -\hat{c}_{rb}$, with initial condition $c_b(t = 0) = 0$. Literature values for D (Table 1) were used for GAG and collagen (Dimicco and Sah, 2003; Silver and Trelstad, 1980) and D for COMP was estimated from 500 kDa dextran (Leddy et al., 2004). The synthesis rate was evaluated from $\hat{c}_{\text{syn}} = (m_c + m_m)/M$ where M is the molar mass. N_t for GAG and collagen were set roughly equal to the average day 45 concentration of the supplementation group with the highest GAG and collagen content, respectively, and N_t for COMP was equal to 10 times the day 45 concentration of the group with the highest COMP concentration; at these levels the matrix accumulated in a linear fashion, as observed experimentally. With these parameters taken as constants, k_f and k_r for each constituent were determined by a custom MATLAB optimization wrapper code that matched the experimental matrix release pattern over 45 days to the computationally predicted matrix release.

Human Patella-Sized Construct

As an illustration of the applicability of the binding and synthesis constants, we attempted to reproduce the results of a previous CTE study on the culture of a human patella-sized construct, which analyzed the spatial GAG deposition over 35 days of culture (Hung et al., 2003; Hung et al., 2004). This simulation accounted for nutrient limitations due to the large construct size. To perform this computational simulation, it was first necessary to determine the glucose consumption rate and glucose concentration required to sustain tissue growth for this system. Glucose consumption was measured experimentally by assaying the media glucose concentrations of constructs cultured over 7 weeks. Glucose concentration threshold was determined by culturing constructs in media with different glucose supplementation concentrations and measuring ECM deposition after 6 weeks. Further details of these additional experiments are included in the Supplementary Material.

Statistics

Briefly, biochemical and mechanical data were compared via analysis of variance (Tukey's post-hoc test). Further statistical treatments descriptions are supplied in the Supplemental Material.

Results

Mechanical Characterization and Biochemical Composition

Constructs cultured over the 45-day period developed E_Y values that were highest in the β3− group (Figure 2A; $p < 0.001$), consistent with previous studies (Byers et al., 2008; Lima et al., 2007); k was affected by both the course of culture and supplementation (Figure 2B; $p < 0.001$), as was E_T (Figure 2C; $p < 0.001$); by day 42, construct disk volume was significantly influenced by TGF-β3 (Figure 2D; $p < 0.001$) with the most expansion occurring in the β3− group ($p < 0.05$). GAG was highest in the β3− group (Figure 3A; $p \leq 0.022$) and collagen levels in the β3− and β3+ groups were higher than the control on days 28 and 45 (Figure 3B; $p \leq 0.002$). Collagen concentration was statistically similar between the β3− and β3+ groups ($p = 0.619$). Levels of COMP were similarly affected by TGF-β3

NIH-PA Author Manuscript

NIH-PA Author Manuscript

NIH-PA Author Manuscript

supplementation (Figure 3C; $p < 0.001$), with the highest construct COMP concentration observed on day 45 in the β3− group ($p \leq 0.003$), and the highest overall COMP concentration observed in the β3+ group on day 28 ($p \leq 0.028$). Cessation of TGF-β3 supplementation influenced total pyridinoline concentration (Figure 3D; $p < 0.001$) and pyridinoline per collagen was influenced by the presence of TGF-β3 (Figure 3E; $p < 0.001$). Correlations between mechanical and biochemical properties are presented in the Supplementary Material.

Experimental Synthesis Rates and Retention Fractions

GAG, collagen, and COMP levels in constructs and media increased nearly linearly over time (Figure 1), as assessed with the coefficient of determination of the linear regression (R^2; Table 2). Scaffold accumulation rates and media release rates for these constituents were evaluated from the slope of the linear regression. Matrix release into the media exhibited a higher R^2 than the scaffold accumulation. The lowest coefficient of determination was the COMP scaffold accumulation for the β3+ group ($R^2 = 0.37$).

Synthesis rates varied with TGF-β3 supplementation (Figure 4). GAG scaffold accumulation rate was highest in the β3− group ($p < 0.001$) and GAG media release rates were similar between the three supplementation groups ($p = 0.429$). Collagen scaffold accumulation rate was highest in the β3− and β3+ groups compared with the control ($p < 0.001$) and collagen media release rate was lowest in the β3− group ($p = 0.002$). COMP synthesis was low ($\sim 10^2$ $\mu g \cdot (ml \cdot day)^{-1}$) compared to the synthesis of the GAG and collagen (~ 1 $mg \cdot (ml \cdot day)^{-1}$). The β3+ group had the highest COMP media release rate ($p < 0.001$) and the β3− group had the highest COMP scaffold accumulation rate ($p \leq 0.021$).

For all matrix constituents (Figure 5), the β3− group had the highest retention ratio ($p < 0.001$). GAG retention was high ($R_c = 90 \pm 2\%$) in the β3− group. COMP retention was lowest in the β3+ group ($R_c = 7 \pm 2\%$; $p < 0.001$).

Theoretical Model Synthesis Rates and Binding Kinetics

Curve-fitting of finite element models of small constructs against matrix accumulation and media release profiles yielded estimates of k_f and k_r and reproduced the experimental set-up over the 45 day culture of the system (representative profile in Figure 6), showing mostly high correlations (Table 1). Synthesis rate for each constituent and group was assumed constant, consistent with the data. The reversible binding parameters for a single constituent varied little with supplementation compared with the variations among the different constituents. These parameters predicted bound constituent concentrations that were reduced at the periphery and homogenous within the interior of the tissue (representative result in Figure S1B of bound GAG in the β3− group).

Human Patella-Sized Construct

Tissue engineering simulations of a patella-sized construct used the measured glucose consumption rate of $1.24 \pm 0.35 \times 10^{-13}$ mol $cell^{-1}$ hr^{-1} and a glucose threshold of 12.5 mM (Supplementary Material), values consistent with prior reports (Marcus and Srivasta, 1973; Obradovic et al., 1999). The large construct model predicted glucose concentrations within

NIH-PA Author Manuscript

NIH-PA Author Manuscript

NIH-PA Author Manuscript

the construct interior falling below the 12.5 mM threshold for the majority of the time in culture (Figure 7A, B, C). Due to this reduced glucose availability, bound GAG developed solely in the periphery when modeling nutrient-dependent synthesis (Figure 7E, F). This example qualitatively agrees with our previous experimental findings (Figure 7F from this study to Figure 7H from Hung, et al. 2004).

Discussion

Engineering cartilage constructs large enough to replace defects seen in symptomatic OA requires scaling up the current size of constructs. Presently, thicker and wider constructs experience heterogeneous matrix deposition as steep gradients in nutrient availability develop between the construct's periphery and interior due to cellular consumption and diffusion limitations (Bian et al., 2009; Hung et al., 2003; Leddy et al., 2004). Computational modeling of the culture conditions may serve as an essential and cost-effective method for determining the efficacy of techniques aimed at enhancing the functional ECM homogeneity. This study measured the synthesis and binding parameters of small [bovine chondrocyte]-[agarose gel] constructs cultured with sufficient media, obviating severe nutrient heterogeneity within the construct. These results were then combined with our prior work that identified glucose as a critical nutrient for this CTE system to model the culture of a human patella-sized construct (Cigan et al., 2013; Hung et al., 2003).

The synthesis rates of all the molecules examined were affected by TGF-β3 supplementation (Figure 4). In the experimental part of this study GAG synthesis rate was constant during the 45-day culture of constructs (Figure 1 and Table S1), suggesting a constant GAG synthesis model was appropriate here. In contrast, other models of GAG synthesis were based on results suggesting that high GAG content leads to GAG synthesis inhibition (Bruckner et al., 1989; Buschmann et al., 1992; Sandy et al., 1980). Such a phenomenon may be explained by inadequate nutrition and was not observed here with constructs given sufficient nutrients. GAG synthesis was elevated by supplementation of TGF-β3 versus control levels, and was further boosted by terminating the supplementation after 14 days (β3− group). This withdrawal not only increased the total synthesis rate of GAG, as shown previously (Byers et al., 2008; Lima et al., 2007), but also increased GAG retention over the continuous treatment group (~90% retention in the β3− compared with ~75% retention in the β3+ group). This trend in retention was similar to the trend in the dissociation constants (0.14 μM for the β3− group versus 10 μM for the control). A similar experimental K_d (0.22 μM) has been reported for reversible binding between aggrecan and hylauronate (Watanabe et al., 1997). Previous models of GAG binding kinetics in cartilage have been primarily focused on the binding and degradation of PGs in native cartilage (Dimicco and Sah, 2003). These studies used an experimentally determined binding rate between PGs and hyaluronate (Sandy et al., 1989). The two measures of GAG binding affinity (this study: $2 – 73 \times 10^{-9}$ $mM^{-1}s^{-1}$; previously: 1.2×10^{-5} s^{-1}) can be reconciled, however, by multiplying the rate constant by the density of binding sites (300 mM). This 'effective forward binding rate' ($N_t k_f$=$0.06 – 2.22 \times 10^{-5}$ s^{-1}) is similar to previous work. It should also be noted that this study assumed reversible binding as suggested by studies on the binding of aggrecan and

NIH-PA Author Manuscript

NIH-PA Author Manuscript

NIH-PA Author Manuscript

hyaluronate (Watanabe et al., 1997), while the prior work resolubilized PG by degradation, preventing PG from re-binding (Dimicco and Sah, 2003).

TGF-β3 increased collagen synthesis over control, although termination of supplementation did not subsequently alter the total synthesis rate. This observation suggests that TGF-β3 primes the chondrocytes for greater collagen synthesis but is not needed continuously, as chondrocytes retain a memory of this exposure; similar behavior has been observed in fibroblasts (Varga et al., 1987). Both supplementation groups also have a high retention ratio (Figure 5) potentially due to TGF-β3 upregulating small PGs, such as decorin and fibromodulin (Burton-Wurster et al., 2003; Roughley, 2001). Prior studies have analyzed the binding of PGs with collagen (Obrink, 1973a, b; Obrink et al., 1975); specifically, K_d of the collagen-PG interaction is on the order of 30 – 1000 nM under low osmotic conditions (Obrink et al., 1975). This study predicts K_d between 0.2 – 387 nM. As reaching native levels of collagen remains a problem in CTE, these results suggest that increasing collagen content will be more greatly impacted by techniques that increase total collagen synthesis (Eleswarapu and Athanasiou, 2013) rather than those which solely increase construct retention (Grogan et al., 2003).

COMP synthesis was stimulated by TGF-β3. In contrast to GAG and collagen, COMP synthesis does not appear to retain a memory of past exposure to TGF-β3 and was elevated only in the presence of exogenous TGF-β3; studies of superficial chondrocytes have also demonstrated COMP expression and synthesis are upregulated in response to TGF-β (Motaung et al., 2011; Recklies et al., 1998). Despite the high COMP synthesis of the β3+ group, retention was much lower than that of GAG and collagen, resulting in much of the COMP (~93%) to be released into the media. Earlier studies have shown that COMP binds to both aggrecan and chondroitin sulfate under Ca^{2+} concentrations similar to those present in the culture media used in this study K_d ~ 73 nM with heparin, K_d >10 μM with keratan sulfate, and K_d ~10^2 nM with chondroitin sulfates (Chen et al., 2007)). COMP has also been observed to bind with type II collagen, K_d = 1.5 nM, although the conditions under which binding is favorable (2 mM Zn^{2+}) were not present in this study; (Rosenberg et al., 1998). In our theoretical model, K_d ranged from 0.23 to 2.4 nM.

COMP levels have rarely been measured quantitatively in engineered cartilage constructs, thus these results offer a novel finding that merits closer analysis. By day 45 the COMP content in the β3− group was 0.09 ± 0.02 %ww, approaching native levels (native healthy/OA: ~0.4 %ww; rheumatoid arthritis: ~0.1 %ww; (DiCesare et al., 1996)). Despite this similarity, a strong correlation between COMP levels and compressive mechanical properties was not observed (Figure S4C). Additionally, COMP content did not show a strong correlation to construct growth (Figure S4G).

Pyridinoline, while not synthesized directly by cells, was also measured (Figure 3D, E). Pyridinoline is a mature cross-link connecting multiple collagen triple helices; these bonds spontaneously form between hydroxylysine residues in the collagen triple helix (Eyre et al., 1984). Previous studies on engineered cartilage have reported that pyridinoline content typically falls below that seen in native tissue (Riesle et al., 1998; Yan et al., 2009). This study presents the first quantitative assessment of pyridinoline content in the [bovine

NIH-PA Author Manuscript

NIH-PA Author Manuscript

NIH-PA Author Manuscript

chondrocyte]-[agarose gel] system. While the total pyridinoline content was below that typically seen in calf bovine cartilage (~98 nmol/g), the ratio of pyridinoline to collagen was similar to native calf bovine cartilage (~0.46 mol/mol; (Williamson et al., 2003a)). The constructs in this study displayed a moderate correlation between pyridinoline content and E_Y (Figure S4D); similar correlations have been observed in native tissue (Williamson et al., 2003a; Williamson et al., 2003b; Yan et al., 2009). These results suggest that cross-linking occurs at native levels relative to collagen (Figure 3E) and therefore the low pyridinoline content (Figure 3D) of the construct may suffer from low substrate (collagen) concentrations. As suggested from the correlation between E_T and pyridinoline content (Figure S4L), and demonstrated recently (Makris et al., 2013), engineered cartilage mechanical properties may benefit from techniques used to increase cross-linking density.

The model presented here extends previous models that have examined ECM synthesis and nutrient consumption (Chung and Ho, 2010; Dimicco and Sah, 2003; Nikolaev et al., 2010; Obradovic et al., 2000; Sengers et al., 2004a; Sengers et al., 2004b, 2005; van Donkelaar et al., 2011). In the model employed here, glucose was selected as the limiting nutrient. In order to customize these models to optimize tissue culture of anatomically-sized constructs, model parameters must be customized for each CTE system. Two critical sets of parameters of the current model are (a) the synthesis rates and retention of the ECM constituents and (b) the essential nutrients which limit ECM. This study provides the matrix synthesis and binding parameters and glucose consumption rates for the [agarose gel]-[bovine chondrocyte] system, identifying a local glucose threshold concentration of 12.5 mM as a requirement for tissue growth and a glucose consumption rate similar to other chondrocyte-scaffold systems. As an illustration of the use of these parameters, we predicted GAG distribution throughout a human patella-sized construct and compared it to a prior experiment (Hung et al., 2003; Hung et al., 2004). The similarities between the model simulations and experimental results suggest that these models can have great predictive power for the optimization of culture conditions for large constructs.

The modeling aspect of this study focused on the elaboration of ECM constituents and did not account for the mechanical changes associated with enhanced ECM deposition, as done with other cartilage growth models (Khoshgoftar et al., 2013; Nikolaev et al., 2010; Sengers et al., 2004b). Moreover, simplifying assumptions of the model, which neglects ECM degradation or the influence of ECM density on transport properties and ECM synthesis, may not remain valid for other CTE systems or over longer culture durations (Buschmann et al., 1992; Dimicco and Sah, 2003; Leddy et al., 2004).

The findings of this study will inform our ongoing modeling investigations on the optimal density and placement of nutrient channels for engineering large tissue constructs with homogeneous material properties, based on our earlier experimental finding of the effectiveness of such channels (Bian et al., 2009). Further experimental validations of these model predictions will be conducted using a reduced set of configurations identified from the optimization analyses.

NIH-PA Author Manuscript

NIH-PA Author Manuscript

NIH-PA Author Manuscript

Supplementary Material

Refer to Web version on PubMed Central for supplementary material.

Acknowledgments

Research reported in this publication was supported by the National Institute of Arthritis and Musculoskeletal and Skin Diseases (Award Numbers R01AR060361 and R01AR046568), the National Institute of General Medical Sciences (Award Number R01GM083925) of the National Institutes of Health, and the Columbia University Presidential Fellowship. The content is solely the responsibility of the authors and does not necessarily represent the official views of the National Institutes of Health.

References

Ateshian GA. On the theory of reactive mixtures for modeling biological growth. Biomechanics and Modeling in Mechanobiology. 2007; 6:423–445. [PubMed: 17206407]

Ateshian GA, Maas S, Weiss JA. Multiphasic finite element framework for modeling hydrated mixtures with multiple neutral and charged solutes. J Biomech Eng. 2013; 135:111001–111011. [PubMed: 23775399]

Benya PD, Shaffer JD. Dedifferentiated chondrocytes reexpress the differentiated collagen phenotype when cultured in agarose gels. Cell. 1982; 30:215–224. [PubMed: 7127471]

Bian L, Angione SL, Ng KW, Lima EG, Williams DY, Mao DQ, Ateshian GA, Hung CT. Influence of decreasing nutrient path length on the development of engineered cartilage. Osteoarthritis and Cartilage. 2009; 17:677–685. [PubMed: 19022685]

Bruckner P, Horler I, Mendler M, Houze Y, Winterhalter KH, Eich-Bender SG, Spycher MA. Induction and prevention of chondrocyte hypertrophy in culture. J Cell Biol. 1989; 109:2537–2545. [PubMed: 2808534]

Buckley CT, Thorpe SD, Kelly DJ. Engineering of Large Cartilaginous Tissues Through the Use of Microchanneled Hydrogels and Rotational Culture. Tissue Engineering Part A. 2009; 15:3213–3220. [PubMed: 19374490]

Burton-Wurster N, Liu W, Matthews GL, Lust G, Roughley PJ. TGF beta 1 and biglycan, decorin, and fibromodulin metabolism in canine cartilage. Osteoarthritis and Cartilage. 2003; 11:167–176. [PubMed: 12623288]

Buschmann MD, Gluzband YA, Grodzinsky AJ, Kimura JH, Hunziker EB. Chondrocytes in agarose culture synthesize a mechanically functional extracellular matrix. J Orthop Res. 1992; 10:745–758. [PubMed: 1403287]

Byers BA, Mauck RL, Chiang IE, Tuan RS. Transient exposure to transforming growth factor beta 3 under serum-free conditions enhances the biomechanical and biochemical maturation of tissue-engineered cartilage. Tissue Eng Part A. 2008; 14:1821–1834. [PubMed: 18611145]

Chen FH, Herndon ME, Patel N, Hecht JT, Tuan RS, Lawler J. Interaction of cartilage oligomeric matrix protein/thrombospondin 5 with aggrecan. J Biol Chem. 2007; 282:24591–24598. [PubMed: 17588949]

Chung CA, Ho SY. Analysis of collagen and glucose modulated cell growth within tissue engineered scaffolds. Ann Biomed Eng. 2010; 38:1655–1663. [PubMed: 20069364]

Cigan AD, Nims RJ, Albro MB, Esau JD, Dreyer MP, Vunjak-Novakovic G, Hung CTPD, Ateshian GA. Insulin, Ascorbate and Glucose Have a Much Greater Influence than Transferrin and Selenous Acid on the in vitro Growth of Engineered Cartilage in Chondrogenic Media. Tissue Engineering Part A. 2013

Davisson T, Kunig S, Chen A, Sah R, Ratcliffe A. Static and dynamic compression modulate matrix metabolism in tissue engineered cartilage. Journal of Orthopaedic Research. 2002a; 20:842–848. [PubMed: 12168676]

Davisson T, Sah RL, Ratcliffe A. Perfusion increases cell content and matrix synthesis in chondrocyte three-dimensional cultures. Tissue Eng. 2002b; 8:807–816. [PubMed: 12459059]

NIH-PA Author Manuscript

NIH-PA Author Manuscript

NIH-PA Author Manuscript

DiCesare PE, Carlson CS, Stolerman ES, Hauser N, Tulli H, Paulsson M. Increased degradation and altered tissue distribution of cartilage oligomeric matrix protein in human rheumatoid and osteoarthritic cartilage. Journal of Orthopaedic Research. 1996; 14:946–955. [PubMed: 8982138]

Dimicco MA, Sah RL. Dependence of cartilage matrix composition on biosynthesis, diffusion, and reaction. Transport in Porous Media. 2003; 50:57–73.

Eleswarapu SV, Athanasiou KA. TRPV4 channel activation improves the tensile properties of self-assembled articular cartilage constructs. Acta Biomaterialia. 2013; 9:5554–5561. [PubMed: 23128162]

Eyre DR, Paz MA, Gallop PM. Cross-Linking in Collagen and Elastin. Annual Review of Biochemistry. 1984; 53:717–748.

Eyre DR, Wu JJ. Collagen cross-links. Top Curr Chem. 2005; 247:207–229.

Grogan SP, Rieser F, Winkelmann V, Berardi S, Mainil-Varlet P. A static, closed and scaffold-free bioreactor system that permits chondrogenesis in vitro. Osteoarthritis and Cartilage. 2003; 11:403–411. [PubMed: 12801480]

Hedbom E, Antonsson P, Hjerpe A, Aeschlimann D, Paulsson M, Rosa-Pimentel E, Sommarin Y, Wendel M, Oldberg A, Heinegard D. Cartilage matrix proteins. An acidic oligomeric protein (COMP) detected only in cartilage. J Biol Chem. 1992; 267:6132–6136. [PubMed: 1556121]

Hung CT, Lima EG, Mauck RL, Takai E, LeRoux MA, Lu HH, Stark RG, Guo XE, Ateshian GA. Anatomically shaped osteochondral constructs for articular cartilage repair. J Biomech. 2003; 36:1853–1864. [PubMed: 14614939]

Hung CT, Mauck RL, Wang CC, Lima EG, Ateshian GA. A paradigm for functional tissue engineering of articular cartilage via applied physiologic deformational loading. Annals of Biomedical Engineering. 2004; 32:35–49. [PubMed: 14964720]

Jurvelin J, Saamanen AM, Arokoski J, Helminen HJ, Kiviranta I, Tammi M. Biomechanical properties of the canine knee articular cartilage as related to matrix proteoglycans and collagen. Eng Med. 1988; 17:157–162. [PubMed: 3224734]

Kempson GE, Muir H, Pollard C, Tuke M. The tensile properties of the cartilage of human femoral condyles related to the content of collagen and glycosaminoglycans. Biochim Biophys Acta. 1973; 297:456–472. [PubMed: 4267503]

Khoshgoftar M, Wilson W, Ito K, van Donkelaar CC. Influence of tissue- and cellscale extracellular matrix distribution on the mechanical properties of tissue-engineered cartilage. Biomech Model Mechanobiol. 2013; 12:901–913. [PubMed: 23160844]

Langer R, Vacanti JP. Tissue engineering. Science. 1993; 260:920–926. [PubMed: 8493529]

Leddy HA, Awad HA, Guilak F. Molecular diffusion in tissue-engineered cartilage constructs: effects of scaffold material, time, and culture conditions. J Biomed Mater Res B Appl Biomater. 2004; 70:397–406. [PubMed: 15264325]

Lima EG, Bian L, Ng KW, Mauck RL, Byers BA, Tuan RS, Ateshian GA, Hung CT. The beneficial effect of delayed compressive loading on tissue-engineered cartilage constructs cultured with TGF-beta3. Osteoarthritis Cartilage. 2007; 15:1025–1033. [PubMed: 17498976]

Maas SA, Ellis BJ, Ateshian GA, Weiss JA. FEBio: finite elements for biomechanics. Journal of Biomechanical Engineering. 2012; 134:011005. [PubMed: 22482660]

Makris EA, MacBarb RF, Responte DJ, Hu JC, Athanasiou KA. A copper sulfate and hydroxylysine treatment regimen for enhancing collagen cross-linking and biomechanical properties in engineered neocartilage. FASEB J. 2013; 27:2421–2430. [PubMed: 23457219]

Marcus RE, Srivasta VML. Effect of Low Oxygen Tensions on Glucose-Metabolizing Enzymes in Cultured Articular Chondrocytes. Proceedings of the Society for Experimental Biology and Medicine. 1973; 143:488–491. [PubMed: 4267770]

Mauck RL, Soltz MA, Wang CC, Wong DD, Chao PH, Valhmu WB, Hung CT, Ateshian GA. Functional tissue engineering of articular cartilage through dynamic loading of chondrocyte-seeded agarose gels. Journal of Biomechanical Engineering. 2000; 122:252–260. [PubMed: 10923293]

Moisio K, Eckstein F, Chmiel JS, Guermazi A, Prasad P, Almagor O, Song J, Dunlop D, Hudelmaier M, Kothari A, Sharma L. Denuded Subchondral Bone and Knee Pain in Persons With Knee Osteoarthritis. Arthritis and Rheumatism. 2009; 60:3703–3710. [PubMed: 19950284]

NIH-PA Author Manuscript

NIH-PA Author Manuscript

NIH-PA Author Manuscript

Motaung SCKM, Di Cesare PE, Reddi AH. Differential response of cartilage oligomeric matrix protein (COMP) to morphogens of bone morphogenetic protein/transforming growth factor-beta family in the surface, middle and deep zones of articular cartilage. Journal of Tissue Engineering and Regenerative Medicine. 2011; 5:E87–E96. [PubMed: 21604381]

Nikolaev NI, Obradovic B, Versteeg HK, Lemon G, Williams DJ. A Validated Model of GAG Deposition, Cell Distribution, and Growth of Tissue Engineered Cartilage Cultured in a Rotating Bioreactor. Biotechnology and Bioengineering. 2010; 105:842–853. [PubMed: 19845002]

Obradovic B, Carrier RL, Vunjak-Novakovic G, Freed LE. Gas exchange is essential for bioreactor cultivation of tissue engineered cartilage. Biotechnology and Bioengineering. 1999; 63:197–205. [PubMed: 10099596]

Obradovic B, Meldon JH, Freed LE, Vunjak-Novakovic G. Glycosaminoglycan deposition in engineered cartilage: Experiments and mathematical model. Aiche Journal. 2000; 46:1860–1871.

Obrink B. The influence of glycosaminoglycans on the formation of fibers from monomeric tropocollagen in vitro. European Journal of Biochemistry. 1973a; 34:129–137. [PubMed: 4267112]

Obrink B. A study of the interactions between monomeric tropocollagen and glycosaminoglycans. European Journal of Biochemistry. 1973b; 33:387–400. [PubMed: 4266508]

Obrink B, Laurent TC, Carlsson B. The binding of chondroitin sulphate to collagen. FEBS Letters. 1975; 56:166–169. [PubMed: 1157930]

Recklies AD, Baillargeon L, White C. Regulation of cartilage oligomeric matrix protein synthesis in human synovial cells and articular chondrocytes. Arthritis and Rheumatism. 1998; 41:997–1006. [PubMed: 9627009]

Riesle J, Hollander AP, Langer R, Freed LE, Vunjak-Novakovic G. Collagen in tissue-engineered cartilage: Types, structure, and crosslinks. Journal of Cellular Biochemistry. 1998; 71:313–327. [PubMed: 9831069]

Rosenberg K, Olsson H, Morgelin M, Heinegard D. Cartilage oligomeric matrix protein shows high affinity zinc-dependent interaction with triple helical collagen. Journal of Biological Chemistry. 1998; 273:20397–20403. [PubMed: 9685393]

Roughley PJ. Articular cartilage and changes in arthritis: noncollagenous proteins and proteoglycans in the extracellular matrix of cartilage. Arthritis Res. 2001; 3:342–347. [PubMed: 11714388]

Sandy JD, Brown HL, Lowther DA. Control of proteoglycan synthesis. Studies on the activation of synthesis observed during culture of articular cartilages. Biochem J. 1980; 188:119–130. [PubMed: 6773523]

Sandy JD, O'Neill JR, Ratzlaff LC. Acquisition of hyaluronate-binding affinity in vivo by newly synthesized cartilage proteoglycans. Biochemical Journal. 1989; 258:875–880. [PubMed: 2730571]

Sengers BG, Oomens CW, Baaijens FP. An integrated finite-element approach to mechanics, transport and biosynthesis in tissue engineering. Journal of Biomechanical Engineering. 2004a; 126:82–91. [PubMed: 15171133]

Sengers BG, Van Donkelaar CC, Oomens CW, Baaijens FP. The local matrix distribution and the functional development of tissue engineered cartilage, a finite element study. Annals of Biomedical Engineering. 2004b; 32:1718–1727. [PubMed: 15675683]

Sengers BG, van Donkelaar CC, Oomens CW, Baaijens FP. Computational study of culture conditions and nutrient supply in cartilage tissue engineering. Biotechnol Prog. 2005; 21:1252–1261. [PubMed: 16080709]

Silver FH, Trelstad RL. Type I collagen in solution. Structure and properties of fibril fragments. Journal of Biological Chemistry. 1980; 255:9427–9433. [PubMed: 7410433]

Stockwell, RA. Biology of cartilage cells. Cambridge University Press; Cambridge: 1979.

van Donkelaar CC, Chao G, Bader DL, Oomens CW. A reaction-diffusion model to predict the influence of neo-matrix on the subsequent development of tissue-engineered cartilage. Comput Methods Biomech Biomed Engin. 2011; 14:425–432. [PubMed: 21516527]

Varga J, Rosenbloom J, Jimenez SA. Transforming growth factor beta (TGF beta) causes a persistent increase in steady-state amounts of type I and type III collagen and fibronectin mRNAs in normal human dermal fibroblasts. Biochem J. 1987; 247:597–604. [PubMed: 3501287]

NIH-PA Author Manuscript

NIH-PA Author Manuscript

NIH-PA Author Manuscript

Watanabe H, Cheung SC, Itano N, Kimata K, Yamada Y. Identification of hyaluronan-binding domains of aggrecan. Journal of Biological Chemistry. 1997; 272:28057–28065. [PubMed: 9346959]

Williamson AK, Chen AC, Masuda K, Thonar EJMA, Sah RL. Tensile mechanical properties of bovine articular cartilage: variations with growth and relationships to collagen network components. Journal of Orthopaedic Research. 2003a; 21:872–880. [PubMed: 12919876]

Williamson AK, Masuda K, Thonar EJMA, Sah RL. Growth of immature articular cartilage in vitro: Correlated variation in tensile biomechanical and collagen network properties. Tissue Engineering. 2003b; 9:625–634. [PubMed: 13678441]

Yan D, Zhou GD, Zhou X, Liu W, Zhang WJ, Luo XS, Zhang L, Jiang T, Cui L, Cao YL. The impact of low levels of collagen IX and pyridinoline on the mechanical properties of in vitro engineered cartilage. Biomaterials. 2009; 30:814–821. [PubMed: 19036435]

Zhou S, Cui Z, Urban JP. Nutrient gradients in engineered cartilage: metabolic kinetics measurement and mass transfer modeling. Biotechnol Bioeng. 2008; 101:408–421. [PubMed: 18727036]

NIH-PA Author Manuscript
NIH-PA Author Manuscript
NIH-PA Author Manuscript

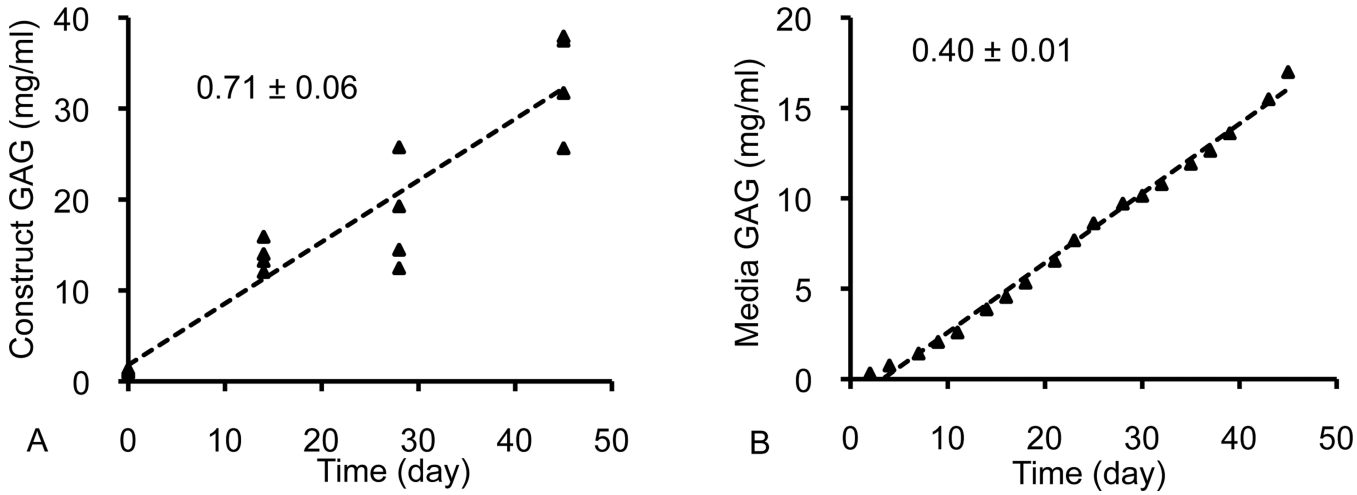

Figure 1.

Representative synthesis profiles for (A) matrix accumulation in the construct and (B) cumulative matrix release in the media. Synthesis rates were calculated from the slope of the linear regression.

NIH-PA Author Manuscript

NIH-PA Author Manuscript

NIH-PA Author Manuscript

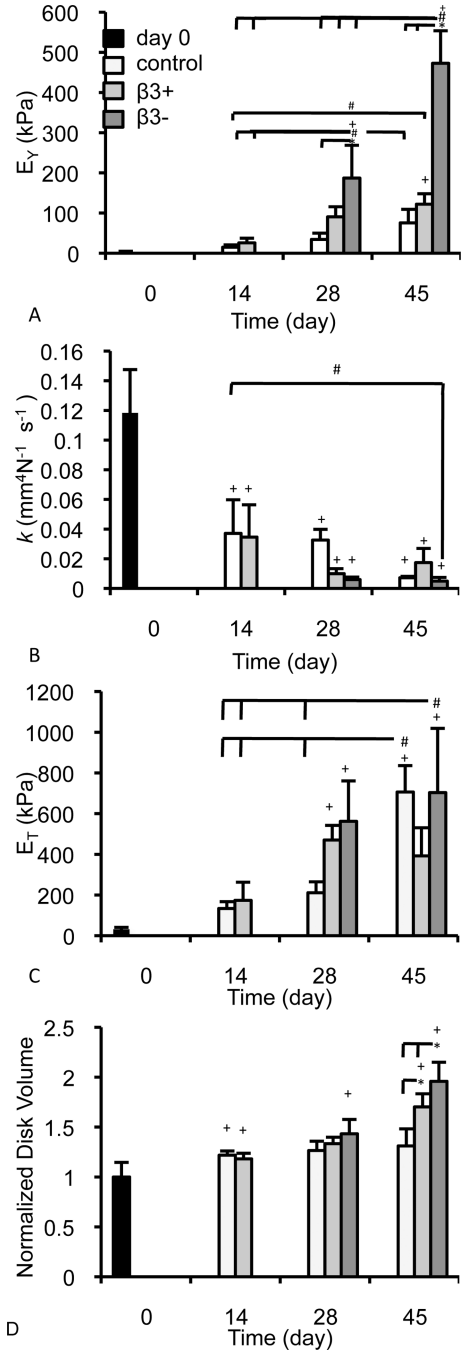

Figure 2.

Curve-fit mechanical properties (A) E_Y (kPa), (B) k (mm^4 N^{-1} s^{-1}), (C) E_T (kPa) and (D) the experimentally determined normalized disk volume of constructs over the course of culture. * denotes group significantly differ from indicated group(s) at same time point ($p < 0.05$); + denotes group significantly differ from day 0 properties ($p < 0.05$); # denotes the indicated groups differ significantly ($p < 0.05$).

NIH-PA Author Manuscript
NIH-PA Author Manuscript
NIH-PA Author Manuscript

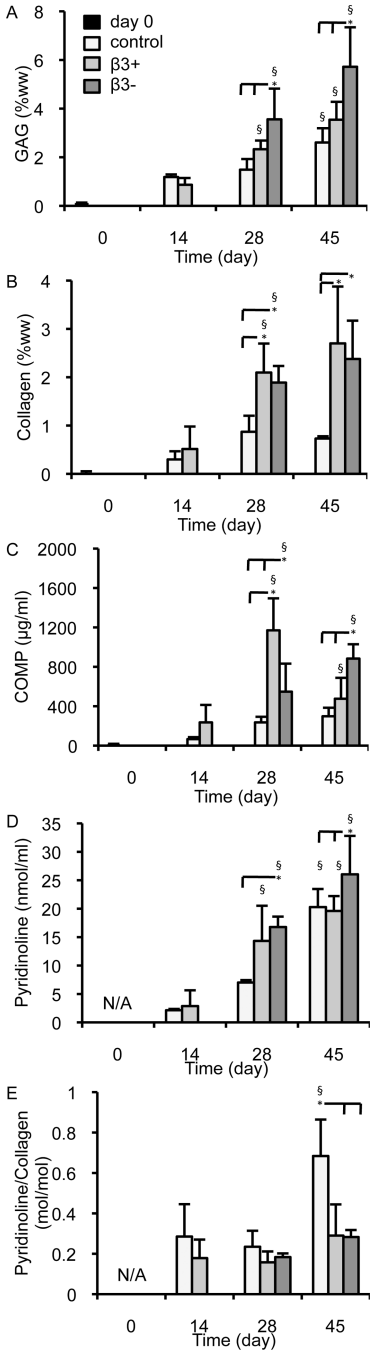

Figure 3.

Biochemical properties of constructs over the culture period: (A) GAG concentration (%ww), (B) collagen concentration (%ww), (C) COMP concentration (μg/ml), (D) pyridinoline concentration (nmol/ml), and (E) pyridinoline to collagen ratio (mol/mol). * denotes group significantly differ from indicated group(s) at same time point ($p < 0.05$); § denotes group significantly differ from previous time point ($p < 0.05$; day 7 control and β3+ compared to day 0 and day 28 β3+ and β3− compared to day 14 β3+).

NIH-PA Author Manuscript

NIH-PA Author Manuscript

NIH-PA Author Manuscript

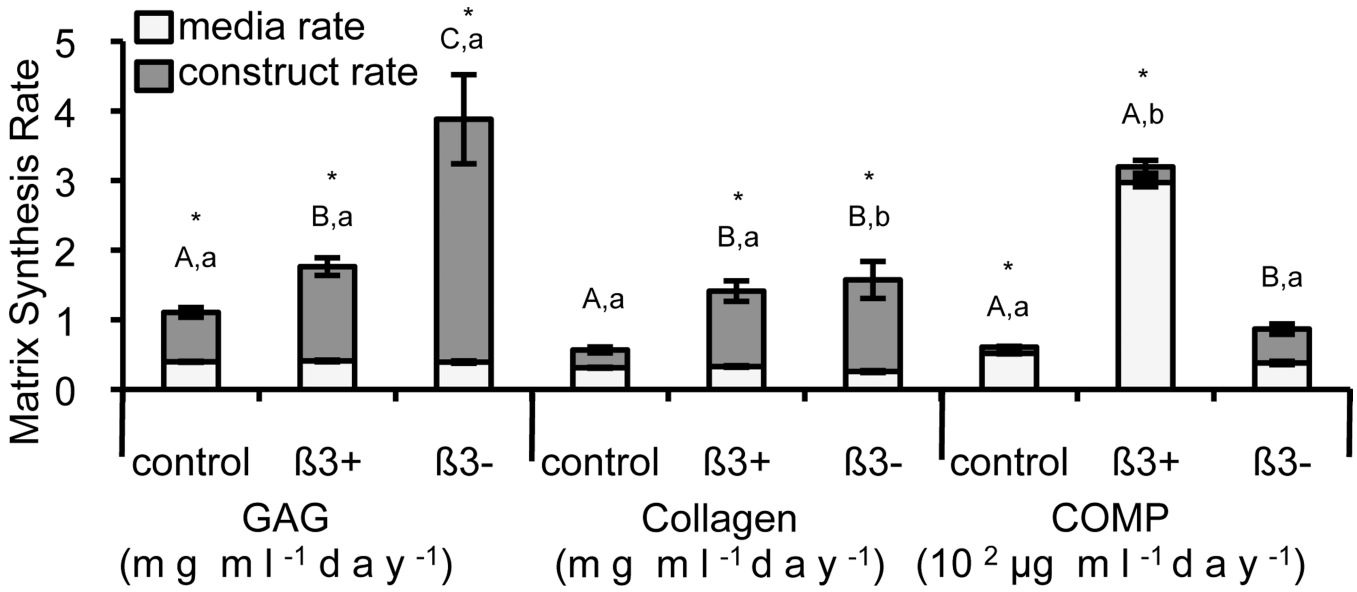

Figure 4.

Synthesis rates of GAG (mg $ml^{-1}day^{-1}$), collagen (mg $ml^{-1}day^{-1}$), and COMP (10^2 µ*g* $ml^{-1}day^{-1}$). The total synthesis (total column) is divided between media release rate (light, bottom) and construct accumulation rate (dark, top). * denotes significant differences between media and construct synthesis rates ($p < 0.05$); upper case letters denote groups of significance of construct accumulation for each matrix constituent ($p < 0.05$) and lower case letters denote groups of significance of media release for each matrix constituent ($p < 0.05$); thus for each matrix constituent, groups with the same upper or lower case letters had statistically similar construct matrix accumulation or matrix media release, respectively.

NIH-PA Author Manuscript

NIH-PA Author Manuscript

NIH-PA Author Manuscript

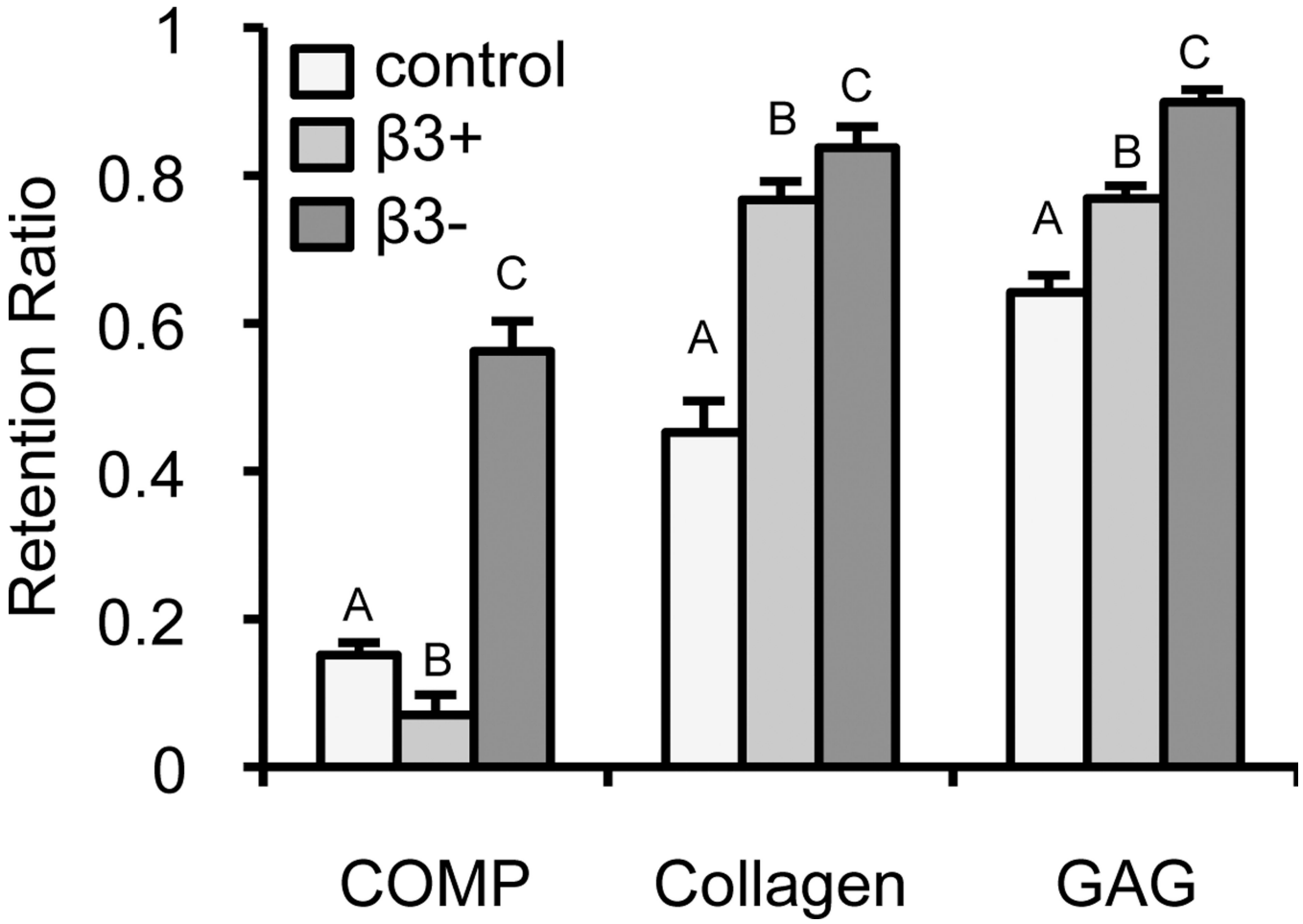

Figure 5.

Retention ratio of the matrix constituents COMP, collagen, and GAG for each of the TGF-β3 culture treatments: control (light), β3+ (medium), and β3− (dark). Upper case letters denote groups of significance ($p < 0.05$); thus for each matrix constituent: groups with different capital letters were statistically different.

NIH-PA Author Manuscript
NIH-PA Author Manuscript
NIH-PA Author Manuscript

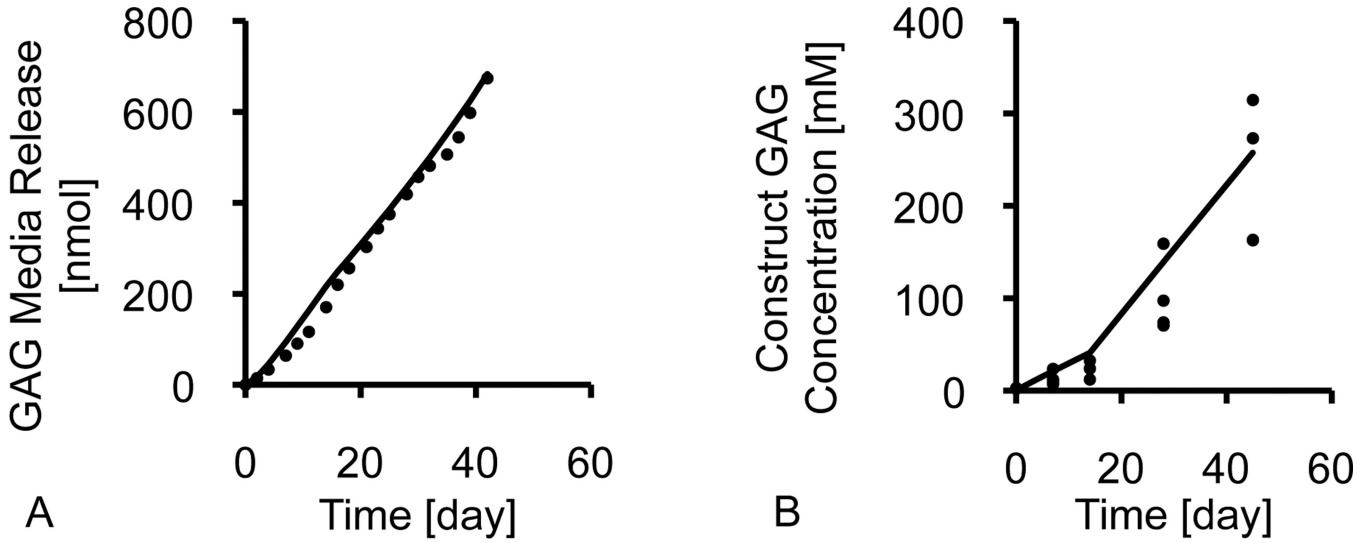

Figure 6.

Representative (A) cumulative media release and (B) construct accumulation experimental data (circles) and the theoretical model results (line) of the GAG constituent in the β3− group. The inflection at day 14 in (B) reflects changes in synthesis rate and binding kinetics associated with TGF-β3 cessation.

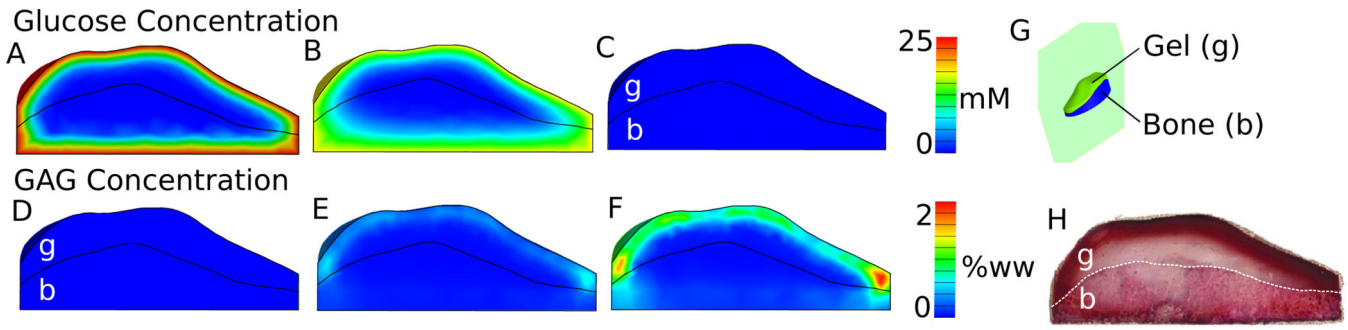

Figure 7.

Model simulation results (sagittal plane, G) of the glucose concentration distributions (A, B, C) and bound GAG distribution (D, E, F) in patella-sized CTE construct (cellular gel region, “g”, and the cellular gel + porous bone scaffold, “b”) during the 35 days of culture. Simulations were based on prior experimental work and the GAG synthesis and binding parameters were taken from the ‘control’ parameters measured in this study. Glucose distribution images are (A) 1 hr, (B) 12 hrs, and (C) 71 hr after a media change. GAG distribution images are on (D) day 0, (E) day 17, and (F) day 35. The previous experimental results of GAG accumulation (saffarin-O stained histological slices) after 35 days of culture (H) are provided for comparison to the model simulations (F) of this study. (H) from (Hung et al., 2004) with kind permission from Springer Science and Business Media.

NIH-PA Author Manuscript NIH-PA Author Manuscript NIH-PA Author Manuscript

NIH-PA Author Manuscript
NIH-PA Author Manuscript
NIH-PA Author Manuscript

Table 1

GAG, collagen, and COMP transport and reversible binding parameters for the computational model: diffusion coefficients, in free solution, D_o, and within the construct, D, partition coefficient, κ, matrix binding site density within the tissue, N_t, forward, k_f, and reverse, k_r, binding constants, dissociation constant, K_d, and the model fits of the experimental matrix accumulation, $R^2_{construct}$, and media release, R^2_{media}, profiles.

Constituent	Parameter	Control	β3+	β3−
GAG	$D_o^{GAG}(\mathrm{mm^2 s^{-1}})$	1×10^{-7}	1×10^{-7}	1×10^{-7}
	D^{GAG} (mm² s⁻¹)	5×10^{-8}	5×10^{-8}	5×10^{-8}
	κ^{GAG}	1	1	1
	$N_t^{GAG}(\mathrm{mM})$	300	300	300
	$k_f^{GAG}(\mathrm{mM^{-1}s^{-1}})$	2.0×10^{-9}	9.1×10^{-9}	7.4×10^{-8}
	$k_r^{GAG}(\mathrm{s^{-1}})$	2.1×10^{-11}	1.2×10^{-11}	1.0×10^{-11}
	$K_d^{GAG}(\mathrm{mM})$	1.1×10^{-2}	1.3×10^{-3}	1.3×10^{-4}
	R^2_{media}	0.99	0.99	0.99
	$R^2_{construct}$	0.89	0.89	0.85
Collagen	$D_o^{col}(\mathrm{mm^2 s^{-1}})$	4.5×10^{-6}	4.5×10^{-6}	4.5×10^{-6}
	D^{col} (mm² s⁻¹)	2.25×10^{-6}	2.25×10^{-6}	2.25×10^{-6}
	κ^{col}	1	1	1
	$N_t^{col}(\mathrm{mM})$	0.3	0.3	0.3
	$k_f^{col}(\mathrm{mM^{-1}s^{-1}})$	4.4×10^{-5}	5.8×10^{-4}	9.7×10^{-4}
	$k_r^{col}(\mathrm{s^{-1}})$	4.0×10^{-9}	2.3×10^{-7}	1.5×10^{-10}
	$K_d^{col}(\mathrm{mM})$	9.1×10^{-5}	4.0×10^{-4}	1.6×10^{-7}
	R^2_{media}	0.99	0.99	0.99
	$R^2_{construct}$	0.72	0.81	0.69
COMP	$D_o^{COMP}(\mathrm{mm^2 s^{-1}})$	6.6×10^{-4}	6.6×10^{-4}	6.6×10^{-4}
	D^{COMP} (mm² s⁻¹)	3.3×10^{-4}	3.3×10^{-4}	3.3×10^{-4}
	κ^{COMP}	1	1	1

NIH-PA Author Manuscript

NIH-PA Author Manuscript

NIH-PA Author Manuscript

Constituent	Parameter	Control	β3+	β3−
	$N_t^{COMP}(\mathrm{mM})$	0.04	0.04	0.04
	$k_f^{COMP}(\mathrm{mM}^{-1}\mathrm{s}^{-1})$	1.7×10^{-3}	1.2×10^{-3}	6.3×10^{-3}
	$k_r^{COMP}(\mathrm{s}^{-1})$	4.1×10^{-9}	8.8×10^{-10}	1.5×10^{-9}
	$K_d^{COMP}(\mathrm{mM})$	2.4×10^{-6}	7.3×10^{-7}	2.4×10^{-7}
	R^2_{media}	0.99	0.99	0.98
	$R^2_{construct}$	0.83	0.35	0.82

NIH-PA Author Manuscript
NIH-PA Author Manuscript
NIH-PA Author Manuscript

Table 2

Coefficients of determination (R^2) and p-values (p) for the linear regression fits to the construct matrix accumulation ("Accumulation") and cumulative matrix release ("Release") over the course of culture (control and β3+ regressions over days 0 to 45; β3− regression over day 14 to 45).

Constituent		Group					
		β3−		β3+		Control	
		R^2	p	R^2	p	R^2	p
GAG	Accumulation	0.77	<0.001	0.90	<0.001	0.89	<0.001
	Release	0.98	<0.001	0.98	<0.001	0.99	<0.001
Collagen	Accumulation	0.69	<0.001	0.82	<0.001	0.72	<0.001
	Release	0.97	<0.001	0.98	<0.001	0.99	<0.001
COMP	Accumulation	0.81	<0.001	0.37	0.007	0.84	<0.001
	Release	0.95	<0.001	0.99	<0.001	0.99	<0.001